Effect of PKCβ on Retinal Oxygenation Response in Experimental Diabetes

Hongmei Luan,[1] *Michael Leitges,*[2] *Rita R. Gupta,*[1] *Daniel Pacheco,*[1] *Andres Seidner,*[1] *Jessica Liggett,*[1] *Yasuki Ito,*[1] *Renu Kowluru,*[3] *and Bruce A. Berkowitz*[1,3]

Purpose. To test the hypotheses that, in mice, breathing carbogen (95% O_2-5% CO_2) oxygenates the retina better than breathing 100% oxygen, the superior hemiretinal oxygenation response to carbogen inhalation is subnormal early in diabetes, and diabetes-induced elevation of retinal protein kinase C (PKC)-β contributes to this pathophysiology.

Methods. Retinal oxygenation response (ΔPo_2) was measured using functional magnetic resonance imaging (MRI) and either carbogen or 100% oxygen inhalation challenge in C57BL/6J control (C) mice. Retinal ΔPo_2 during carbogen breathing was also measured in PKCβ knockout (C57BL6-Prkcb1; [KO]), 4 month C57BL/6J diabetic (D), and 4-month diabetic PKCβ KO (D+KO) mice. Retinal PKCβ protein expression was assessed by Western analysis.

Results. In C mice, retinal ΔPo_2 during carbogen breathing was significantly greater ($P < 0.05$) than during oxygen breathing. In D mice, ΔPo_2 during carbogen breathing was significantly lower than normal in the superior, but not the inferior, hemiretina and was normal ($P > 0.0$ 5) in the KO group. In the D+KO mice ΔPo_2 was normal ($P > 0.05$) only at distances less than 1.5 mm from the optic nerve head. PKCβ expression was elevated in the retina in diabetes ($P < 0.05$), but was significantly decreased ($P < 0.05$) in D+KO mice.

Conclusions. The present study confirms that, in the mouse, retinal ΔPo_2 patterns during different inhalation challenges or in the presence of diabetes are similar to what has been reported in rats. Diabetes-induced elevation of PKC appears to contribute only focally to subnormal retinal ΔPo_2. This raises the possibility that PKC inhibition therapy may be only regionally effective in treating retinal pathophysiology associated with diabetic retinopathy. (*Invest Ophthalmol Vis Sci.* 2004; 45:937–942) DOI:10.1167/iovs.03-1007

Identifying diabetes-related biochemical changes in the retina that are associated with early pathophysiology and subsequent histopathology could pinpoint potential targets for therapeutic intervention. The activity of protein kinase C (PKC), a key regulator of diverse phenotypic activity, including cell growth and differentiation, is elevated in the retina of diabetic and galactose-fed rodents.[1–4] In particular, elevated expression of the PKCβ isoform has been implicated in decreased steady state retinal perfusion after 2 weeks of diabetes in the rat.[4,5] It is not yet known whether increased PKCβ expression regulates functional aspects of retinal circulatory pathophysiology associated with longer durations of diabetes.

We have developed a novel functional magnetic resonance imaging (MRI) method for measuring the retinal oxygenation response to a hyperoxic inhalation challenge in the newborn and adult rat, rabbit, cat, and human.[6–11] In this technique, hyperoxia-induced increases in vitreous partial oxygen pressure over the room-air value (ΔPo_2) are measured as increased signal intensity. Good agreement is found between the MRI-measured response and that derived from oxygen electrode data in normal rat retina under similar conditions.[12,13] In control rats, during a carbogen challenge, oxygen from the choroid is mostly consumed by the inner plexiform layer and does not enter the preretinal vitreous space to a substantial degree.[12,14] A number of interrelated hemodynamic parameters can modulate oxygen supply during a carbogen challenge, including retinal vessel autoregulation, perfusion reserve, ocular perfusion pressure, plasma pH, and vascular density. In normal adult and newborn rats, carbogen breathing oxygenates the retina significantly better than pure oxygen breathing.[13] Carbogen, a gas mixture of carbon dioxide (5%) and oxygen (95%), is used clinically instead of 100% oxygen to minimize the vasoconstrictive effects of pure O_2 on retinal blood flow and oxygenation.

Application of this functional MRI method in rat models of diabetic retinopathy has revealed that the superior hemiretina exhibits a lesser (i.e., subnormal) oxygenation response than is found in control (i.e., normal) animals and that this abnormality appears several months before retinal histopathology becomes apparent.[7,15] In principle, during a carbogen challenge, reduced oxygen supplied by the retinal circulation and/or increased retinal oxygen consumption could produce a subnormal response. However, a subnormal oxygenation response does not appear to represent retinal hypoxia.[16] Because retinal oxygen demand may decrease in experimental diabetes,[17,18] our working hypothesis is that measurement of a subnormal retinal ΔPo_2 is primarily a measure of a decrease in oxygen supplied by the retinal circulation.[6–8,15]

Aminoguanidine (AMG), a compound shown to inhibit retinal PKC activity in diabetes, preserved the retinal oxygenation response at the 3-month time point and prevented the development of retinal histopathology at 15 months of diabetes in rats.[2,15,19] In contrast, AMG treatment of galactose-fed rats did not protect the retinal oxygenation response at 3 months, nor did it prevent the development of retinal lesions at 15 months.[7,15,19,20] Galactose-fed rats treated with an aldose reductase inhibitor also preserved the retinal oxygenation response and prevented development of retinal lesions.[15] Taken together, these data underscore the use of retinal ΔPo_2 measurements as a potential surrogate marker of the efficacy of treatment in diabetic retinopathy.

In this study, we examined whether in the mouse retinal ΔPo_2 patterns during breathing of carbogen and oxygen as well

From the Departments of [1]Anatomy and Cell Biology and [3]Ophthalmology, Wayne State University, Detroit, Michigan; and [2]Max-Planck-Institut für Experimental Endokrinologie, Hannover, Germany.

Supported by National Eye Institute Grant R01 EY10221, Research to Prevent Blindness, and the Juvenile Diabetes Research Foundation International.

Submitted for publication September 11, 2003; revised November 21, 2003; accepted December 1, 2003.

Disclosure: **H. Luan**, None; **M. Leitges**, None; **R.R. Gupta**, None; **D. Pacheco**, None; **A. Seidner**, None; **J. Liggett**, None; **Y. Ito**, None; **R. Kowluru**, None; **B.A. Berkowitz**, None

The publication costs of this article were defrayed in part by page charge payment. This article must therefore be marked "*advertisement*" in accordance with 18 U.S.C. §1734 solely to indicate this fact.

Corresponding author: Bruce A. Berkowitz, Department of Anatomy and Cell Biology, Wayne State University School of Medicine, 540 E. Canfield, Detroit, MI 48201; baberko@med.wayne.edu.

as in diabetes were similar to those in the rat.[7,13,15] In addition, we began to test the hypothesis that diabetes-induced elevation of PKCβ in the retina contributes to the development of an early subnormal ΔPo_2. Retinal ΔPo_2 was compared in control, diabetic, and diabetic PKCβ KO mice. Diabetic mice exhibited early biochemical changes, including elevation of PKC activity, similar to those in diabetic rats.[1] Furthermore, in long-term (>15 months) experimental diabetes in mice, retinal histopathology (acellular capillaries and pericyte ghosts) developed that is similar to that observed in lesions in long-term diabetes in rats and early in the course of diabetes in humans.[21–23]

METHODS

The animals were treated in accordance with the NIH Guide for the Care and Use of Laboratory Animals and the ARVO Statement for the Use of Animals in Ophthalmic and Vision Research.

Animal Models

Control (C57BL/6J, C group) mice were purchased from Jackson Laboratories (Bar Harbor, ME) and PKC mice with targeted disruption of the PKCβ gene (KO group) with a C57J background (C57BL6-Prkcb1) were provided by one of the authors (ML).[24] The KO mice have a similar lifespan as the C57BL/6J (Leitges M, personal communication, December 2000).

Diabetes was induced in the C57BL/6J and KO mice (starting weight, 20–24 g) by streptozotocin (65 mg/kg; 50 mM citrate buffer [pH 4.5]) intraperitoneal injection once a day for 5 days. Body weight, blood glucose, and urine ketones levels were monitored weekly. Insulin (neutral protamine Hagedorn [NPH]) was administered to allow slow weight gain while maintaining hyperglycemia (blood glucose levels above 400 mg/dL). Normal rodent chow and water were provided ad libitum. After 4 months of diabetes, only those mice with fasting blood glucose levels higher than 400 mg/dL (D group) were studied by functional MRI.

Western Blot Analysis

Retinal tissue was homogenized in 30 mM Tris-HC buffer containing 10 mM EGTA, 5 mM EDTA, 1% Triton X-100, and 250 mM sucrose containing 1 mM NaF, 1 mM phenylmethylsulfonyl fluoride, 15 μg/mL aprotinin, 5 μg/mL leupeptin, 5 μg/mL pepstatin, and 1 mM Na_3VO_4. The homogenate was centrifuged at 5000*g* for 5 minutes at 4°C to remove cell debris. The protein concentration was determined with the bicinchoninic acid assay (BCA; Sigma-Aldrich, St. Louis, MO) with bovine serum albumin used as the standard. Retinal protein (30–40 μg) was separated on a 10% reducing polyacrylamide gel and then transferred to nitrocellulose membranes. The membranes were blocked in the wash buffer (10 mM Tris-HCl [pH 7.5], 100 mM NaCl and 0.1% Tween 20), containing 5% milk, followed by the incubation with a polyclonal antibody against PKCβ (catalog no. sc-210; Santa Cruz Biotechnology, Santa Cruz, CA) at a dilution of 1:1000. The membranes were washed three times (10 minutes each), and incubated for 1 hour at room temperature with horseradish-peroxidase–linked anti-rabbit Ig (Amersham Pharmacia Biotech, Amersham, UK; 1:2500 dilution), and developed with a Western blot kit (ECL-Plus; Amersham Pharmacia Biotech).

To ensure equal loading among lanes, the expression of the intrinsic protein β-actin was quantified in each lane. The intensities of PKCβII band and β-actin band in each lane were quantified with an automated gel digitizing system (Un-Scan-It; Silk Scientific, Orem, UT). After blots were transferred to the membranes for detection of PKC, the membranes were incubated with stripping buffer (62.5 mM Tris-HCl [pH 6.8], 100 mM mercaptoethanol, and 2% sodium dodecyl sulfate) at 50°C for 30 minutes, washed, and incubated with antibody against β-actin (Sigma-Aldrich). The secondary antibody used was anti-mouse IgG horseradish-peroxidase–conjugated antibody, and the membranes were developed with the Western blot kit (ECL-Plus; Amersham). Each sample was analyzed at least in duplicate.

Functional MRI Examination

On the day of the experiment, anesthesia was induced by a single intraperitoneal injection of urethane (36% solution, 0.083 mL/20 g animal weight, prepared fresh daily; Aldrich, Milwaukee, WI). Each mouse was gently positioned on an MRI-compatible custom-made holder with its nose placed in a plastic nose cone. Animals were allowed to breathe spontaneously during the experiment. To maintain the core temperature, a recirculating heated water blanket was used. Rectal temperature was continuously monitored while the animal was inside the magnet.[15]

MRI data were acquired on a 4.7-T system using a two-turn transmit-and-receive surface coil (1.0 cm diameter) placed over the eye, as previously described[6] (repetition time [TR], 1 second; echo time [TE], 22.7 ms; number of acquisitions [NA], 1; matrix size, 128 × 256; slice thickness, 1 mm; field of view, 18 × 18 mm; sweep width, 25,000 Hz; 2 minutes per image). Examining the initial retinal oxygenation response to a hyperoxic challenge requires careful attention to experimental timing and makes high demands on the animals' physiology, compared with steady state measurements.

The functional MRI data were collected as follows. Sagittal localizer images were first collected and used to position a single 1-mm-thick transverse slice through the center of the eye. The 1-mm slice thickness was needed to obtain an adequate signal-to-noise ratio in a 2-minute image. This slice thickness resulted in some partial volume averaging, so that the final image contained superior and inferior hemiretina, with a relatively minor contribution from the temporal and nasal hemiretina. A capillary tube (1.5-mm inner diameter) filled with distilled water was used as the external standard.

It is important to note that steady state (room air) vitreous oxygen tension cannot be measured by this method, because many factors affect the preretinal vitreous water signal and its relaxation properties. In other words, simply obtaining an image of the eye during room air breathing alone cannot be used to measure retinal oxygenation. In addition, detailed inferences regarding oxygen consumption and delivery in individual retinal layers cannot be made, because functional MRI measures vitreal oxygenation and so reflects general treads in intraretinal oxygenation.[14] Nonetheless, as discussed in the introduction, retinal ΔPo_2 have shown promise as a biomarker of treatment efficacy in diabetic retinopathy.

In general, ΔPo_2 data were collected approximately 90 minutes after urethane injection to avoid potential errors due to variable time under urethane anesthesia. Three images were acquired while the animal breathed room air and one image during the inhalation of carbogen or 100% oxygen. The hyperoxic gas exposure was started at the end of the third image. Animals were returned to room air for 5 minutes to allow recovery from the inhalation challenge and were removed from the magnet. A second 2-minute inhalation challenge was performed outside the magnet with care taken to avoid altering the spatial relationship between the animal head and nose cone. At exactly 2 minutes, arterial blood from the abdominal aorta was collected as described previously.[8] This blood was analyzed for glucose, percentage of glycated hemoglobin, Pao_2, $Paco_2$, and pH. However, because the length of time that the blood was stored before the percent glycated hemoglobin assay, the data produced were not reproducible and so are not reported. Note that this second inhalation challenge (outside the magnet) is needed because it is not feasible to obtain routinely an arterial blood sample from inside the magnet (>40 cm away from the magnet opening) from 25 g mice. In all cases, after the blood collection, the mice were killed with an intracardiac potassium chloride injection and eyes enucleated for Western blot analysis.

Data Analysis

To be included in this study, the animal must have demonstrated (1) minimal eye movement during the MRI examination, (2) a nongasping

respiratory pattern before the MRI examination, (3) rectal temperature in the range of 35.5 to 36.5°C, and (4) Pao_2 higher than 350 mm Hg and $Paco_2$ between 46 and 65 mm Hg during the carbogen challenge. Occasionally, the blood gas machine was not able to read a sample (e.g., due to a clot or excessive air in the capillary tube). In this case, the MRI data were also excluded. Between 5 to 20 animals in each of the different treatment groups satisfied the fourth inclusion criterion.

To correct for possible subtle shifting of the animals' position during the experiment (usually for reasons unrelated to the physiology of the animal, such as settling on the gauze packing) a warp affine image coregistration was performed on each animal with software written in-house. After coregistration, the MRI data were transferred to a computer (Power Mac G4; Apple Computer, Cupertino, CA) and analyzed with the software program Image (available by ftp at zippy.nimh.nih.gov/ or at http://rsb.info.nih.gov/nih-image; developed by Wayne Rasband, National Institutes of Health, Bethesda, MD). Images obtained during room air breathing were averaged to improve the signal-to-noise ratio. All pixel signal intensities in the average-room-air image and the 2-minute carbogen image were then normalized to the external standard intensity. Signal intensity changes during carbogen breathing were calculated and converted to ΔPo_2 values, on a pixel-by-pixel basis, as follows.[13] For each pixel, the fractional signal enhancement (E) was calculated

$$E = (S(t) - S_0)/S_0 \quad (1)$$

where $S(t)$ is the pixel signal intensity at time t after starting the gas inhalation, and S_0 is the control signal intensity (measured from the average of the three control images) at the same pixel spatial location. E values were converted into ΔPo_2 according to a previously established theory[13]

$$\Delta Po_2 = E/(R_1{}^*T_k) \quad (2)$$

where R_1 is the oxygen relaxivity (second^{-1} · mm Hg^{-1}), and $T_k = T_r \cdot \exp^{(-T_r/T_{10})}$, where T_r is the repetition time, and T_{10} is the T_1 in the absence of oxygen. Using a T_r of 1 second and assuming a vitreous T_{10} of 4 seconds, $T_k = 3.52$. This T_{10} value is based on our previous measurement of the proton spin–lattice relaxation time in the rabbit vitreous (4 seconds) and reported values in human vitreous (3.3 seconds) and in cerebral spinal fluid (4.3 seconds), which has a high water content similar to that of vitreous.[13,25] An R_1 of 2×10^{-4} sec^{-1} · mm Hg^{-1} was used.[13] This R_1 was previously measured in a saline phantom, which is assumed to be a reasonable model of vitreous (98% water).[13] A similar R_1 value was found for plasma, suggesting that relatively low protein levels do not substantially contribute to oxygen relaxivity.[26] Note that an E of 0.01 (i.e., a 1% signal intensity change) corresponds to a ΔPo_2 of 14 mm Hg.

The ΔPo_2 parameter image was analyzed as follows: First, the pixel value along a 1-pixel-thick line at the boundary of the retina-choroid and vitreous was set to 255 (black). We estimate that the thickness of this line, based on the in-plane resolution (18×18 mm^2 field of view was sampled by 128×256 data points) of 140×70 μm, is approximately 100 μm. The values in another 1-pixel-thick line drawn in the preretinal vitreous next to the black pixels were then extracted.[6] This procedure minimized retina–choroid pixel values from potentially contaminating those used in the final analysis ("pixel bleed") and insured that similar preretinal vitreous space was sampled for each animal. In addition, spatial averaging over these 100-μm regions of interest tends to minimize the contribution from the very local preretinal oxygenation gradients next to the retinal surface.[27] An average ΔPo_2 band was constructed based on the within-group mean for each pixel. Note that due to the size of our in-plane pixels (approximately 100 μm) and slice thickness, changes in oxygen from regions less than 100 μm, such as a particular retinal artery, cannot be measured. However, inhomogeneous distributions of retinal oxygenation responses on a scale of more than 100 μm are readily observed, when present.

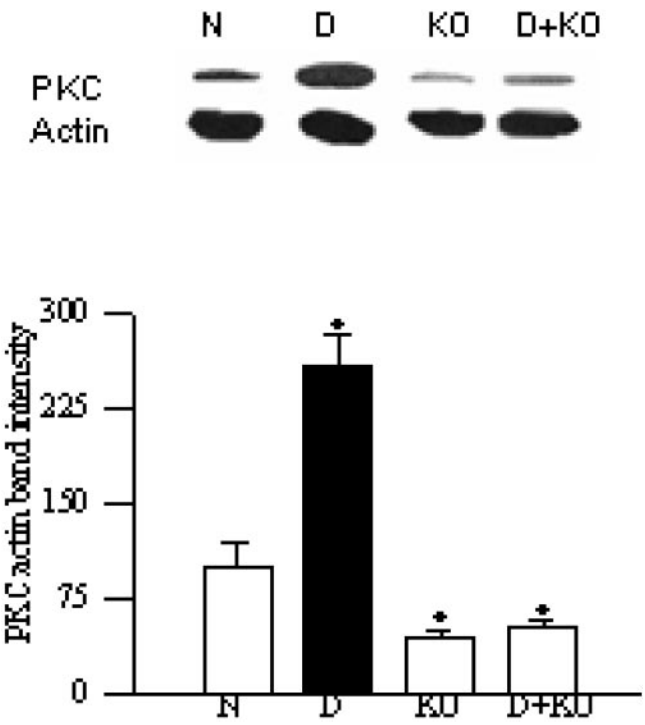

FIGURE 1. Retinal PKCβII expression in control (N) and PKCβ KO (KO) mice made diabetic (4 months D). PKCβII content was determined by Western blot techniques with a polyclonal antibody against PKCβII. The Western blots are representative of four mice in each group. The retina from each mouse was analyzed in duplicate in two separate experiments. The intensities of the PKCβII and β-actin bands in each lane were quantified with an automated digitizing system. The histograpm represents PKCβII band intensity (mean ± SD) from the same mice, adjusted to the intensity of the intrinsic protein β-actin. *Significant differences ($P < 0.05$) compared with the control.

Statistical Analysis

The physiological parameters (i.e., blood gas values, rectal temperatures, blood glucose data) were normally distributed and are presented as the mean ± SEM. Comparisons were performed with an unpaired t-test. Separate comparisons of retinal ΔPo_2 between the C and D groups and between the KO and D+KO groups were performed with a generalized estimating equation. This method performs a general linear regression analysis using all the pixels in each subject and accounts for the within-subject correlation between adjacent pixels. When multiple comparisons were made, the likelihood of finding a significant impact for all the comparisons by chance alone is $P \leq 0.0167$ (0.05/(number of comparisons made) or 0.05/3 = 0.0167). When two samples were compared, $P \leq 0.05$ was considered significant.

RESULTS

Characterization of Retinal PKCβ Expression

Figure 1 shows Western blots from representative retinal extracts. PKCβ expression was elevated ($P < 0.05$) by more than twofold in the retina of 4-month D mice compared with C mice. The expression of PKCβ in the retina was decreased by approximately 60% in the KO mice and 50% in D+KO mice, compared with the C group ($P < 0.001$). However, no difference ($P > 0.05$) was found in expression between the KO and

TABLE 1. Summary of Mouse Systemic Physiology (mean ± SEM)

Group	Fasting Blood Glucose (mg/dL)	During Carbogen Challenge			
		Pao_2 (mm Hg)	$Paco_2$ (mm Hg)	pH	Core Temperature (°C)
C carbogen (n = 20)	131 ± 13	551 ± 13	59 ± 1	7.19 ± 0.00	35.7 ± 0.1
C oxygen (n = 6)	128 ± 19	617 ± 15*	39 ± 1*	7.32 ± 0.02*	36.1 ± 0.2
4-Mo D carbogen (n = 13)	520 ± 30*	587 ± 17	53 ± 2	7.23 ± 0.02	35.8 ± 0.1
KO carbogen (n = 9)	126 ± 12	569 ± 14	57 ± 2	7.22 ± 0.03	36.4 ± 0.2
D+KO carbogen (n = 5)	522 ± 42*	593 ± 8	56 ± 2	7.24 ± 0.01	35.6 ± 0.2

* Significantly different from C carbogen group, $P \leq 0.05$.

D+KO groups. As shown in Figure 1, despite the significant differences in the content of PKCβ among various lanes, the content of β-actin was not significantly different.

Systemic Physiology

A summary of the mouse blood glucose, core temperature, and blood parameters measured during the 2-minute hyperoxic challenges are presented in Table 1. As expected, the C group breathing carbogen had higher ($P < 0.05$) $Paco_2$ and lower pH levels than mice breathing 100% oxygen. Pao_2 levels were different ($P < 0.05$) between carbogen and oxygen breathing. We think that the large differences in $Paco_2$ and pH between carbogen and oxygen breathing explains the larger increase in retinal ΔPo_2 during carbogen breathing (Fig. 2) better than the small Pao_2 difference (approximately 10%). Compared with C-group mice, all D-group animals had significantly ($P < 0.05$) elevated blood glucose levels. There were no significant ($P > 0.05$) differences in plasma glucose levels between the D and D+KO groups. The Pao_2, pH, and core temperature were not significantly ($P > 0.05$) different among any of the carbogen-breathing mouse groups (Table 1).

Functional MRI

We and others have demonstrated in rats that carbogen breathing produces a larger retinal oxygenation response than that produced by 100% oxygen breathing.[12,13] In different groups of control mice, we confirmed that 2 minutes of carbogen breathing (panretinal ΔPo_2 = 142 ± 4, n = 20) produced a larger ($P < 0.05$) oxygenation response than during oxygen inhalation (panretinal ΔPo_2 = 78 ± 5, n = 6; Fig. 2). Further experiments in the present study were performed with carbogen gas to best detect subtle differences in retinal oxygenation between groups.

Figure 3 summarizes the retinal ΔPo_2 data in all groups. No significant ($P > 0.05$) differences were found between the superior and inferior hemiretinal ΔPo_2 of the control and PKC KO mice (i.e., no hemiretinal asymmetry) or between the inferior hemiretinal ΔPo_2 in all the groups. A significantly ($P < 0.05$) subnormal average superior hemiretinal ΔPo_2 was found only in the D group.

Figure 4 summarizes the superior hemiretina pixel ΔPo_2 versus distance from the optic nerve head for the C, D, KO, and D+KO groups. No significant differences ($P > 0.05$) were found between the inferior hemiretinal ΔPo_2 in any of these groups (data not shown). Although the pansuperior hemiretinal ΔPo_2 of the D+KO mice was not subnormal compared with the KO group ($P > 0.05$, Fig. 3), retinal ΔPo_2 was normal only in a region less than 1.5 mm from the optic nerve head.

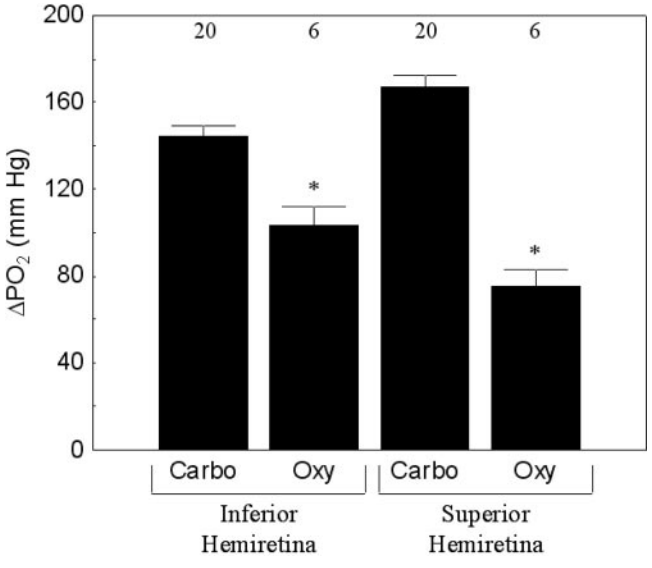

FIGURE 2. Inferior and superior hemiretinal ΔPo_2 in control mice breathing either carbogen (Carbo) or 100% oxygen (Oxy). Both hemiretinal responses during oxygen breathing were lower than during carbogen breathing (*$P < 0.05$). The number of animals used to generate these data is listed above each histogram. Error bars, SEM.

DISCUSSION

In this study, we confirmed that the pattern of the mouse retinal response to carbogen and 100% oxygen breathing are

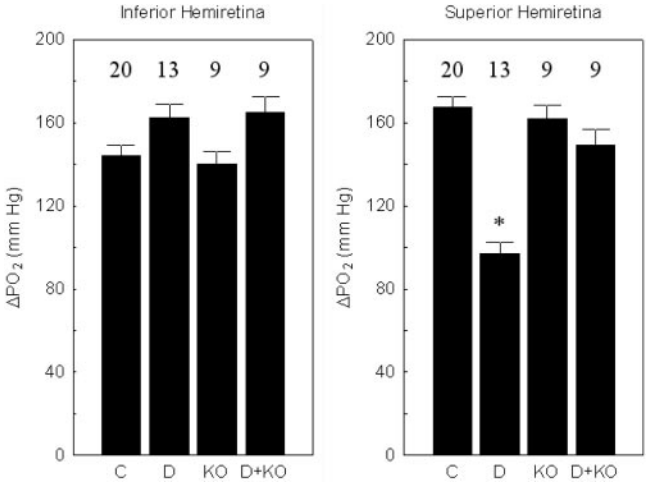

FIGURE 3. Histograms of (*left*) inferior and (*right*) superior hemiretinal ΔPo_2 in the C and D groups. The inferior hemiretinal ΔPo_2s were not significantly ($P > 0.05$) different between any groups. A subnormal (*$P < 0.05$) superior hemiretinal ΔPo_2 was found only in the D group. The number of animals used to generate these data is listed above each histogram. Error bars, SEM.

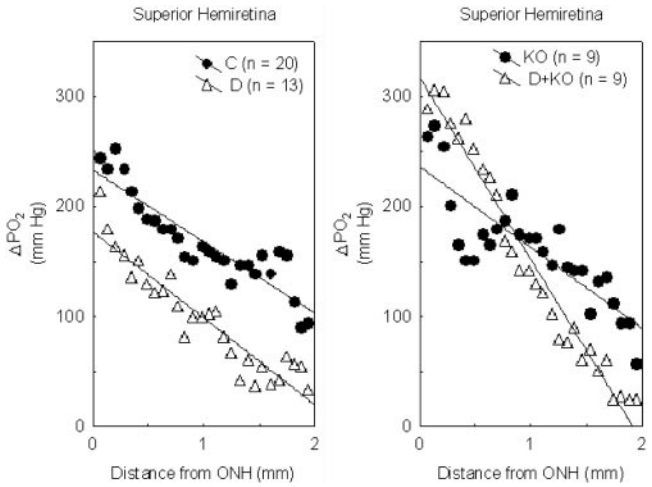

FIGURE 4. Plots of the average superior hemiretina pixel ΔPo_2 versus distance from the optic nerve head for combined C and D groups (*left*) and for the C and D+KO groups (*right*).

similar to our previous findings in rats.[13] In addition, we measured a pathophysiologic retinal response pattern (subnormal pansuperior hemiretinal ΔPo_2) after 4 months of diabetes in the mouse that was similar to that in the rat with 3 months of experimental diabetes.[7,15] This pathophysiology occurs earlier than the reported development of retinal vascular lesions (acellular capillaries and pericyte ghosts appear at later times [>15 months] in experimental diabetes in mice).[21–23] The mechanism(s) underlying the early superior pathophysiology are not known. It is possible that the present retinal oxygenation differences between the C and D groups were the result of systemic variations between these groups. However, no significant differences in core temperature and blood gas parameters were found (Table 1). Although we did not measure other systemic physiologic parameters, such as blood pressure, it seems reasonable to expect that systemic physiologic differences would similarly affect both the inferior and superior hemiretinal oxygenation response. The lack of differences between the inferior hemiretinal ΔPo_2 in the C and D groups does not support this possibility. Based on these considerations, it appears that the inability of the superior hemiretina to oxygenate in the D group is due to local (i.e., retinal) and not systemic factors.

We have not yet identified any mechanisms that can explain why this early pathophysiology appears in superior but not inferior hemiretina of diabetic rats. In control and KO mice, no superior-inferior hemiretinal ΔPo_2 asymmetry was detected (Fig. 3). One possibility is that early histopathology may preferentially occur in superior hemiretina of diabetic rats. However, to the best of our knowledge, there are no reports of early changes in histology in the superior hemiretina preferentially. However, the relatively small number of lesions in the diabetic retina at more than 15 months prevents finding a statistical answer to this question (Kern T, unpublished data, 2000). Also, superior–inferior differences in choroidal circulation have not been reported, although in the rat, electrode data suggest that oxygen from the choroid is mostly consumed by the photoreceptors and does not enter the preretinal vitreous space.[12] The rodent superior hemiretina is reported to contain a greater number of ganglion cells than the inferior hemiretina and so would be expected to have a relatively greater metabolic demand.[28] We speculate that this greater metabolic demand may make the superior hemiretina more susceptible to a hyperglycemic insult than the inferior hemiretina. Because control and diabetic animals are handled identically throughout the data collection and analysis aspects of the experiment, factors, such as differences in geometry, are similar for both groups of animals. Note that after 15 months of galactose feeding in rats, both superior and inferior hemiretina are subnormal, suggesting that the early superior hemiretinal subnormal response indicates that perhaps the superior region is more susceptible to diabetes-induced damage.[7] The present data in mice, and results from our previous studies in diabetic and galactose-fed rats, highlights a defect in the superior hemiretinal ΔPo_2 as an early marker of diabetes-related histopathology.

Defining the physiology underlying retinal ΔPo_2 remains an area of on-going research. To help clarify interpretation of altered ΔPo_2, we note first that during steady state (room air breathing) conditions, retinal oxygen demand and supply are matched so that all the oxygen delivered to the retina is consumed and none is dumped into the preretinal vitreous. In this case, inner retinal Po_2 is normally maintained by appropriate retinal vasoreactivity over a broad range of ocular perfusion pressures and retinal oxygen consumption rates. However, the retinal circulation is not usually at steady state. Instead, retinal oxygen supply and demand constantly adapt during daily activities. ΔPo_2 is believed to be a measure of how well retinal oxygen supply works. If baseline Po_2 is either higher or lower than normal but ΔPo_2 is normal, the implication is that the circulation will be able to compensate for the baseline abnormality. A subnormal ΔPo_2 (i.e., an inability to match oxygen supply with demand) is expected to have long-term negative consequence for the health of the retina.

In this study, we investigated the contribution of a specific diabetes-induced biochemical abnormality, increased PKCβ activity, to the ΔPo_2 differences between control and D groups.[1] The results of the current work, and the results of others,[2] indicate that retinal PKC expression is elevated before the appearance of retinal histopathology in diabetic and galactose-fed rats and mice (Fig. 1).[1] Increased PKCβ activity can affect retinal circulatory physiology. For example, drug inhibition of PKCβ has been reported to prevent the decreased retinal perfusion measured in the first couple of weeks after conversion to diabetes,[5] attenuate the increase in leukocyte entrapment in the retinal microcirculation during the first 4-week diabetic period in rats,[29] and inhibit preretinal and optic nerve head neovascularization in a nondiabetic branch retinal vein occlusion pig model.[30] As discussed previously, retinal ΔPo_2 is expected to reflect the contributions of a variety of vascular physiological processes, such as vessel autoregulation, that govern the functional retinal oxygenation response during the carbogen challenge.[6] The relationship between decreased steady state perfusion of the retina (as measured using dye dilution methods, for example) and a subnormal functional response to an inhalation provocation has not yet been investigated. We hypothesized that in 4-month D mice, elevated PKCβ contributed to the development of a subnormal ΔPo_2 in experimental diabetic retinopathy.

The results of this study only partially supported this hypothesis. The reported elevated retinal PKCβ activity appears to be important to the development of a subnormal ΔPo_2 in central retina of D mice. To the best of our knowledge there is no literature that maps PKC activity across the mouse retina in normal and KO mice and more work is needed to chart regional PKC in the mouse eye. Our Western blot data show that the protein expression of PKCβ in the retina was decreased by 60% in the KO mice and 50% in the D+KO mice compared with the control mice. This could suggest that the deletion of the gene for PKCβ was incomplete in the retina, or that the polyclonal antibody used for PKCβ was reacting with some other proteins in the retina. However, given that these mice were homozygous for a targeted disruption,[24] the possibility of incomplete PKC knockout in the retina seems unlikely. It

remains to be determined whether or not chronic inhibition of PKCβ in nongenetically altered rodents will correct central retina oxygenation response defects or, more important, prevent long-term retinal histopathology. Nonetheless, these considerations raise the possibility, for the first time, that specific PKCβ inhibition treatment may only be regionally effective in treating retinal pathophysiology associated with diabetic retinopathy.

Acknowledgments

The authors thank Tim Kern for careful reading of this manuscript and suggestions and Robin Roberts for expert assistance and organizational skills.

References

1. Kowluru R. Retinal metabolic abnormalities in diabetic mouse: comparison with diabetic rat. *Curr Eye Res*. 2002;24:123–128.
2. Kowluru RA, Jirousek MR, Stramm L, Farid N, Engerman RL, Kern TS. Abnormalities of retinal metabolism in diabetes or experimental galactosemia: V. Relationship between protein kinase C and ATPases. *Diabetes*. 1998;47:464–469.
3. Kowluru RA, Engerman RL, Case GL, Kern TS. Retinal glutamate in diabetes and effect of antioxidants. *Neurochem Int*. 2001;38:385–390.
4. Shiba T, Inoguchi T, Sportsman RJ, Heath WF, Bursell SE, King GL. Correlation of diacylglycerol level and protein kinase C activity in rat retina to retinal circulation. *Am J Physiol*. 1993;28:E783–E793.
5. Ishii H, Jirousek MR, Koya D, et al. Amelioration of vascular dysfunctions in diabetic rats by an oral PKC beta inhibitor. *Science*. 1996;272:728–731.
6. Berkowitz BA, Zhang W. Significant reduction of the panretinal oxygenation response after 28% supplemental oxygen recovery in experimental ROP. *Invest Ophthalmol Vis Sci*. 2000;41:1925–1931.
7. Berkowitz BA, Kowluru RA, Frank RN, Kern TS, Hohman TC, Prakash M. Subnormal retinal oxygenation response precedes diabetic-like retinopathy. *Invest Ophthalmol Vis Sci*. 1999;40:2100–2105.
8. Berkowitz BA, Penn JS. Abnormal panretinal response pattern to carbogen inhalation in experimental retinopathy of prematurity. *Invest Ophthalmol Vis Sci*. 1998;39:840–845.
9. Berkowitz BA. The role of dissolved plasma oxygen in hyperoxia induced contrast. *Magn Reson Imaging*. 1996;15:123–126.
10. Berkowitz BA, Wilson CA. Quantitative mapping of ocular oxygenation using magnetic resonance imaging. *Magn Reson Med*. 1995;33:579–581.
11. Berkowitz BA, McDonald C, Ito Y, Tofts PS, Latif Z, Gross J. Measuring the human retinal oxygenation response to a hyperoxic challenge using MRI: eliminating blinking artifacts and demonstrating proof of concept. *Magn Reson Med*. 2001;46:412–416.
12. Yu DY, Cringle SJ, Alder V, Su EN. Intraretinal oxygen distribution in the rat with graded systemic hyperoxia and hypercapnia. *Invest Ophthalmol Vis Sci*. 1999;40:2082–2087.
13. Berkowitz BA. Adult and newborn rat inner retinal oxygenation during carbogen and 100% oxygen breathing: comparison using magnetic resonance imaging delta ΔP_{O_2} mapping. *Invest Ophthalmol Vis Sci*. 1996;37:2089–2098.
14. Cringle SJ, Yu DY. A multi-layer model of retinal oxygen supply and consumption helps explain the muted rise in inner retinal PO(2) during systemic hyperoxia. *Comp Biochem Physiol A Mol Integr Physiol*. 2002;132:61–66.
15. Berkowitz BA, Ito Y, Kern TS, McDonald C, Hawkins R. Correction of early subnormal superior hemiretinal ΔPO(2) predicts therapeutic efficacy in experimental diabetic retinopathy. *Invest Ophthalmol Vis Sci*. 2001;42:2964–2969.
16. Zhang W, Ito Y, Berlin E, Roberts R, Berkowitz BA. Role of hypoxia during normal retinal vessel development and in experimental retinopathy of prematurity. *Invest Ophthalmol Vis Sci*. 2003;44:3119–3123.
17. Rimmer TJ, Smith MJ, Ogilvy AJ, McNally PG. Effects of hypoxemia on the electroretinogram in diabetics. *Doc Ophthalmol*. 1996;91:311–321.
18. Sutherland FS, Stefansson E, Hatchell DL, Reiser H. Retinal oxygen consumption in vitro: the effect of diabetes mellitus, oxygen and glucose. *Acta Ophthalmol*. 1990;68:715–720.
19. Kern TS, Tang J, Mizutani M, et al. Response of capillary cell death to aminoguanidine predicts the development of retinopathy: comparison of diabetes and galactosemia. *Invest Ophthalmol Vis Sci*. 2000;41:3972–3078.
20. Frank RN, Amin R, Kennedy A, Hohman TC. An aldose reductase inhibitor and aminoguanidine prevent vascular endothelial growth factor expression in rats with long-term galactosemia. *Arch Ophthalmol*. 1997;115:1036–1047.
21. Hammes HP, Lin J, Renner O, et al. Pericytes and the pathogenesis of diabetic retinopathy. *Diabetes*. 2002;51:3107–3112.
22. Kern TS, Engerman RL. A mouse model of diabetic retinopathy. *Arch Ophthalmol*. 1996;114:986–990.
23. Midena E, Segato T, Radin S, et al. Studies on the retina of the diabetic db/db mouse I. Endothelial cell-pericyte ratio. *Ophthalmic Res*. 1989;21:106–111.
24. Leitges M, Schmedt C, Guinamard R, et al. Immunodeficiency in protein kinase C beta-deficient mice. *Science*. 1996;273:788–791.
25. Ettl A, Fischer-Klein C, Chemelli A, Daxer A, Felber S. Proton relaxation times of the vitreous body in hereditary vitreoretinal dystrophy. *Ophthalmologica*. 1994;208:195–197.
26. Meyer M, Yu O, Eclancher B, Grucker D, Chambron J. NMR relaxation rates and blood oxygenation level. *Magn Reson Med*. 1995;34:234–241.
27. Alder VA, Yu DY, Cringle SJ. Vitreal oxygen tension measurements in the rat eye. *Exp Eye Res*. 1991;52:293–299.
28. Versaux-Bottei C, Martin-Martinelli E, Nguyen-Legros J, Geffard M, Vigny A, Denroy L. Regional specialization of the rat retina: catecholamine-containing amacrine cell characterization and distribution. *J Comp Neurol.* 1986;243:422–433.
29. Nonaka A, Kiryu J, Tsujikawa A, et al. PKC-beta inhibitor (LY333531) attenuates leukocyte entrapment in retinal microcirculation of diabetic rats. *Invest Ophthalmol Vis Sci*. 2000;41:2702–2706.
30. Danis RP, Bingaman DP, Jirousek M, Yang Y. Inhibition of intraocular neovascularization caused by retinal ischemia in pigs by PKCβ inhibition with LY333531. *Invest Ophthalmol Vis Sci*. 1998;39:171–179.